CHAPTER iii

Electromagnetic Analysis [§]

Chapter index

[§]Part of this work has been accepted for publication as: S. Shee, P. Tripathi, and S. Dwivedi, "Dispersion analysis of reltron modulation section and simulation study on the effect of coupling depth on device performance," *IEEE Trans. on Plas. Sci.*, Special Issue on High Power Microwave Generation, doi:10.1109/TPS.2020.3000986

CHAPTER 3

Electromagnetic Analysis

3.1 Introduction

Slow-wave structures (SWSs) are extensively used in microwave amplifiers and oscillators for high power handling capacity and moderate bandwidth. In general, the SWSs are periodic along the direction of wave propagation and symmetric along the azimuth. On the contrary, the side coupled cavity structure used in reltron's modulation section is neither periodic nor symmetric. Hence, the scope of conventional dispersion analysis techniques like the mode matching, or the field matching technique is limited due to the typical geometrical structure that can not be addressed accurately without axis translation. Even after approximating the cylindrical side cavity to the shape of a pie slice, the problem remains quite involved.

This present chapter deals with the derivation of dispersion relation from the equivalent circuit model. A set of circuit equations are formed and arranged as an eigenvalue problem and solved using matrix method. The solutions generate the eigenvalues and the corresponding eigenvectors, leading to the mode designations. Numerical simulations have been carried out to find the normal modes at different coupling depths. From this, the coupling coefficient of the designed modulation section has been calculated.

3.2 Magnetic Coupling in Dominant Pillbox-cavity Mode

The dominant mode in a cylindrical pillbox cavity is TM_{010} mode. The EM field pattern in this mode is similar to TM_{01} waveguide mode with no field variation along the z-axis. The TM modes are characterized by the axial electric field component $E_z \neq 0$. In TM_{010} mode, E_z attains maxima at the cavity axis (Figure 3.1 (a), and (c)), and becomes zero at cavity sidewall following the amplitude profile of zeroth-order Bessel function of the first kind (J_0). The axial magnetic field component $H_z = 0$. However, the radial and the azimuthal components H_ρ and H_ϕ are nonzero, and the general solution in cylindrical geometry gives

$$H_\rho = \frac{j}{k_c^2}\left(\frac{\omega\epsilon}{\rho}\frac{\delta}{\delta\phi}E_z - \beta\frac{\delta}{\delta\rho}H_z\right), \tag{3.1}$$

and

$$H_\phi = \frac{-j}{k_c^2}\left(\omega\epsilon\frac{\delta}{\delta\rho}E_z + \frac{\beta}{\rho}\frac{\delta}{\delta\phi}H_z\right), \tag{3.2}$$

respectively [Pozar (2009)]. Circulation of these nonzero magnetic field components results in an RF current that flows along the inner surface of cavity sidewall, towards (or away from) the center of the end-wall (Figure 3.1 (b), and (d)). The current flow between the top and the bottom end wall in the form of displacement current $\frac{\delta D_z}{\delta t}$ to complete the loop. This kind of oscillation of EM fields is similar to the oscillation of electric and magnetic energy in an LC tank circuit. The metallic end-walls confine the electric field and behave like a capacitor. The surface current flows through the cavity sidewall and constitutes an equivalent inductor in parallel with the capacitor. An aperture along ϕ direction in the sidewall, as in the case of reltron's modulation section, obstructs the flow of the surface current. So, the current gets transformed into a time-varying magnetic field, which eventually results back to surface current in the adjacent cavity. In this way, the first and the second cavity is magnetically coupled through the side coupling cavity.

In gridless reltrons, the beam passes through the annular end walls. The cutoff frequency corresponding to the hole in the annular disc is kept well above the resonant frequency to ensure that no electric coupling occurs at the frequency of operation.

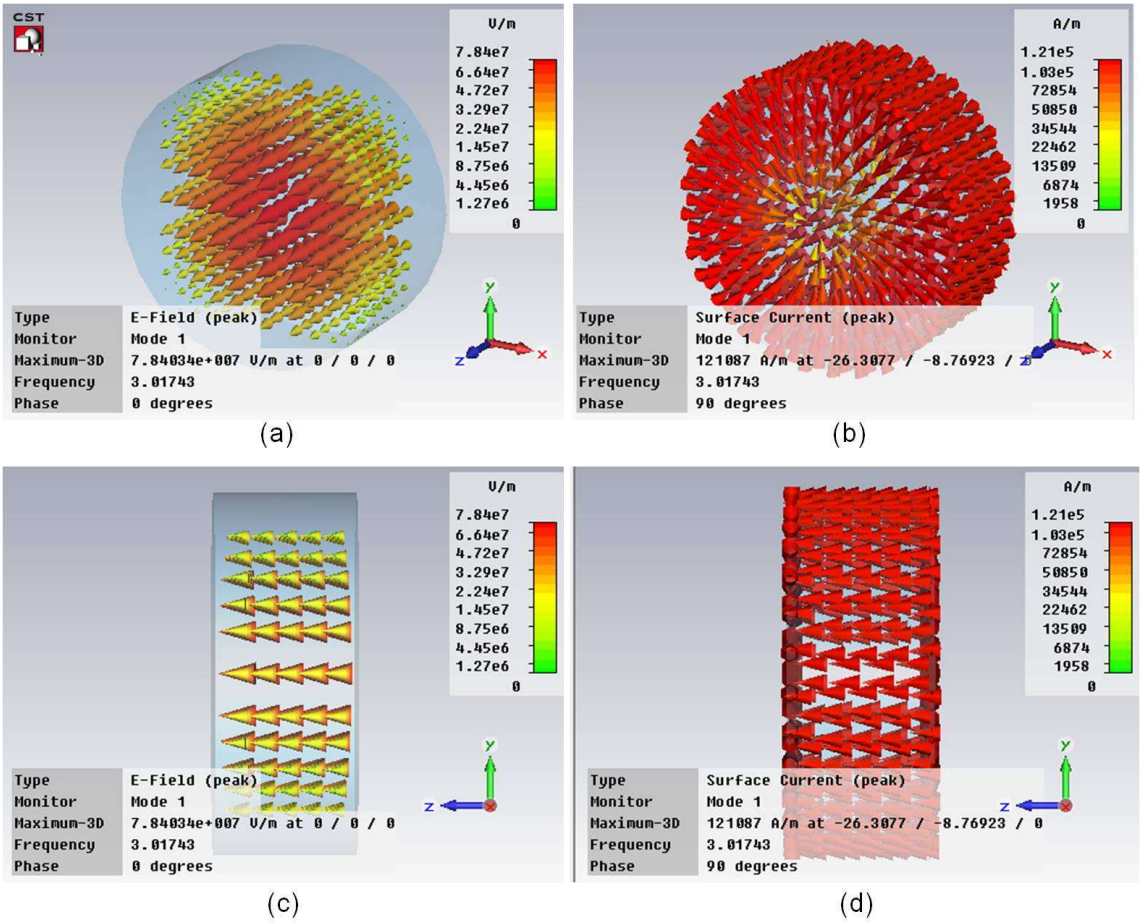

Figure 3.1: Electric field and surface current in dominant TM_{010} mode in a pillbox cavity shown in– (a) and (b) perspective view, (c) and (d) cross-sectional view.

3.3 Normal Modes

In a system of multiple coupled oscillators, normal modes are characterized by the oscillations in which all the elements have the same frequency, i.e., individual oscillators reach their respective extremum as well as cross the zero (or the unexcited state) at the same instant of time.

The normal mode solutions are important because any higher-order mode can be represented by a linear combination of these normal modes.

A system of N numbers of coupled oscillators has N normal modes. So, the reltron's modulation section having three mutually coupled cavities (Figure 3.2), has three normal modes. There are four normal modes in a double side-cavity (DSC) reltron, discussed in Chapter 5.

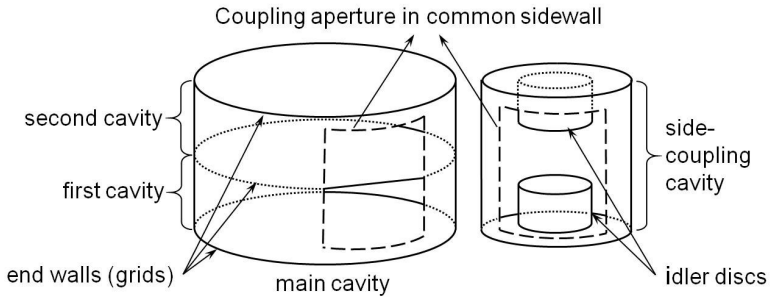

Figure 3.2: Disassembled schematic diagram of reltron modulation section.

3.4 Dispersion Relation from Lumped-element Equivalent Circuit Model

The circuit model of the reltron's modulation section [Soh *et al.* (2010)] is similar to that of a biperiodic side-coupled linear accelerator with a single coupling cell and two on-axis half cells [Knapp *et al,* (1968)]. Three mutually coupled RLC loops represent the three cavities, as shown in Figure 3.3. Here, the mutual inductance $M = kL$, k being the

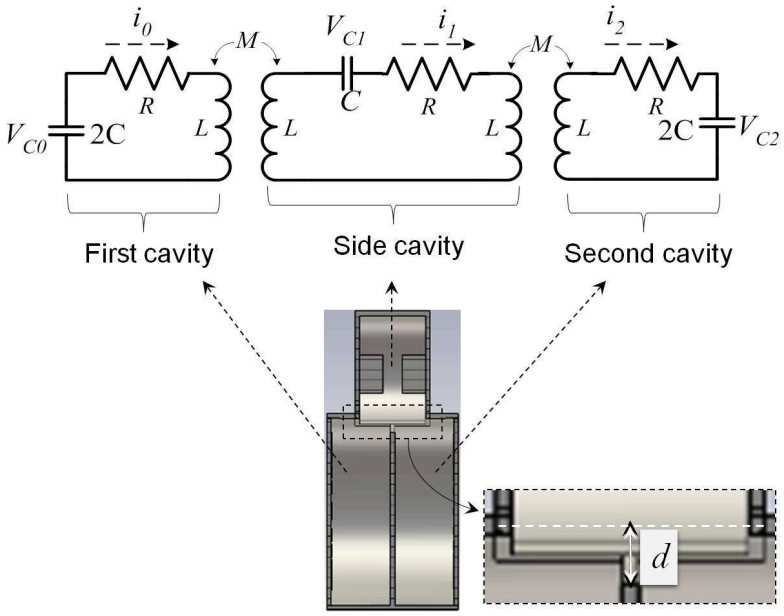

Figure 3.3: Equivalent circuit model of reltron modulation section.

coupling coefficient. No direct coupling exists between the first and the second cavity. Applying Kirchhoff's voltage law in the equivalent circuit of Figure 3.3 in the left, middle,

and the right loop respectively we can write

$$\frac{1}{2C}\int i_0\,dt + i_0R + L\frac{di_0}{dt} - M\frac{di_1}{dt} = 0, \tag{3.3}$$

$$-M\frac{di_0}{dt} + \frac{1}{C}\int i_1 dt + i_1R + L\frac{di_1}{dt} - M\frac{di_2}{dt} = 0, \tag{3.4}$$

and

$$-M\frac{di_1}{dt} + \frac{1}{2C}\int i_2\,dt + i_2R + L\frac{di_2}{dt} = 0. \tag{3.5}$$

Substituting i) $R = 0$, ii) $M = kL$, iii) $i_n = \sqrt{2}I_n e^{j\Omega t}$, where Ω is the frequency of normal mode, iv) $\Phi_n = \sqrt{2}LI_n$, being the magnetic flux in individual cavities $n = 0, 1$ and 2, and v) $\omega_0 = \dfrac{1}{\sqrt{2LC}}$, being the uncoupled resonant frequency; in the above equations we can write

$$\Phi_0\left(1 - \frac{\omega_0^2}{\Omega^2}\right) - k\Phi_1 = 0, \tag{3.6}$$

$$\Phi_1\left(1 - \frac{\omega_0^2}{\Omega^2}\right) - \frac{k}{2}\left(\Phi_0 + \Phi_2\right) = 0, \tag{3.7}$$

and

$$-k\Phi_1 + \Phi_2\left(1 - \frac{\omega_0^2}{\Omega^2}\right) = 0. \tag{3.8}$$

The above equations can be rearranged as

$$\frac{\Phi_0}{\omega_0^2} - k\frac{\Phi_1}{\omega_0^2} = \left(\frac{1}{\Omega^2}\right)\Phi_0, \tag{3.9}$$

$$-k\frac{\Phi_0}{2\omega_0^2} + \frac{\Phi_1}{\omega_0^2} - k\frac{\Phi_2}{2\omega_0^2} = \left(\frac{1}{\Omega^2}\right)\Phi_1, \tag{3.10}$$

and

$$\frac{\Phi_1}{\omega_0^2} - k\frac{\Phi_2}{\omega_0^2} = \left(\frac{1}{\Omega^2}\right)\Phi_2. \tag{3.11}$$

These can be written in matrix form as

$$[W][\Phi_q] = \left(\frac{1}{\Omega^2}\right)[\Phi_q]. \tag{3.12}$$

This is an eigenvalue problem where,

$$[W] = \begin{bmatrix} 1/\omega_0^2 & -k/\omega_0^2 & 0 \\ -k/2\omega_0^2 & 1/\omega_0^2 & -k/2\omega_0^2 \\ 0 & -k/\omega_0^2 & 1/\omega_0^2 \end{bmatrix} \tag{3.13}$$

is the matrix operator which is a function of the cavity resonant frequency ω_0^2 and coupling factor k,

$$[\Phi]_q = \begin{bmatrix} \Phi_0 \\ \Phi_1 \\ \Phi_2 \end{bmatrix} \tag{3.14}$$

is the eigenvector in respective modes $q = 0, 1$, and 2, and $1/\Omega^2$ is the eigenvalue. The diagonal elements of matrix $[W_q]$ represent the resonant oscillation, and the adjacent elements include the effect of coupling. By setting the determinant of $[W_q]$ to zero, we get three eigenvalues that represent the normal mode frequencies

$$\Omega_0 = \frac{\omega_0}{\sqrt{(1+k)}}, \tag{3.15a}$$

$$\Omega_1 = \omega_0, \tag{3.15b}$$

and

$$\Omega_2 = \frac{\omega_0}{\sqrt{(1-k)}}. \tag{3.15c}$$

Substituting these in equation (3.12) we get the corresponding eigenvectors as

$$\Phi_0 = \begin{bmatrix} 1 \\ 1 \\ 1 \end{bmatrix}, \quad \Phi_1 = \begin{bmatrix} -1 \\ 0 \\ 1 \end{bmatrix}, \quad \Phi_2 = \begin{bmatrix} 1 \\ -1 \\ 1 \end{bmatrix}. \tag{3.16}$$

The eigenvectors represent the magnetic flux, which is proportional to the current, and their sign represents the relative direction of their flow in each normal mode. Consequently, the eigenvectors leads to the mode designation as follows– In case of Φ_0, the

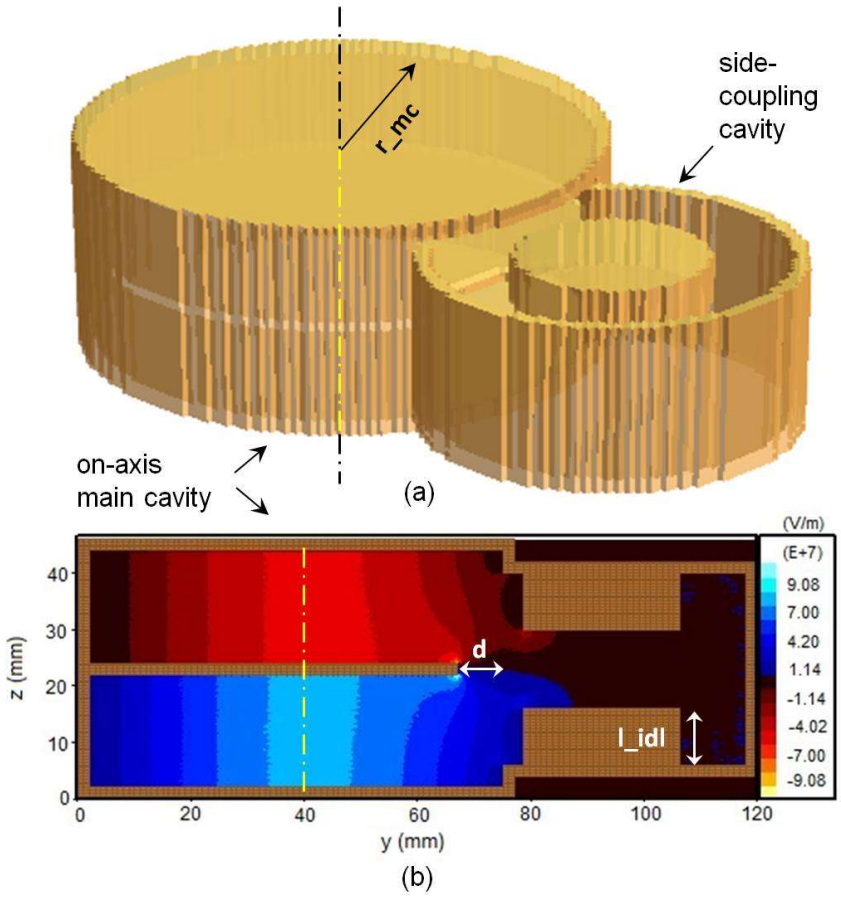

Figure 3.4: (a) Model of reltron modulation section in MAGIC 3D (end wall of the coupling cavity is not shown), and (b) contour plot of $\pi/2$ mode in the cavity cross sectional view along y-z plane.

direction of current in all three loops are the same, corresponding to mode 0. In case of Φ_1, the flow of current is opposite in the first and the third loop, and no current flows in the second loop, corresponding to $\pi/2$ mode. Similarly for Φ_2, current in two consecutive loops flow in opposite direction, corresponding to π mode.

The dispersion relation for a biperiodic coupled-cavity structure, consisting of $N+1$ on-axis cavities with resonant frequency ω_a and N coupling cavities with resonant frequency ω_c, is given by [Miller (2006)]

$$k^2 cos^2\left(\frac{q\pi}{2N}\right) = \left[1-\left(\frac{\omega_a}{\Omega_q}\right)^2\right]\left[1-\left(\frac{\omega_c}{\Omega_q}\right)^2\right], \tag{3.17}$$

where k is the coupling coefficient between the on-axis, and the coupling cavity, $q = 1, 2, .., 2N$, and Ω_q is the frequency of q^{th} normal mode. In reltron's modulation section,

the coupling cavity is placed symmetrically about the midplane of the other two on-axis cavities. So, the above equation can be modified for reltron by substituting $N = 1$ (only one coupling cavity). Now, it gives three equations for the respective normal modes with $q = 0, 1,$ and 2. For $q = 1$ (the $\pi/2$ mode) the coupling cavity remains unexcited, and this equation gives the resonant frequency of the two on-axis cavities as

$$\omega_a = \Omega_1. \tag{3.18}$$

Setting q = 0 and 2 gives two equations containing the two unknowns ω_c and k. The solution gives

$$\omega_c = \sqrt{\frac{2(\Omega_0\Omega_2)^2}{(\Omega_0^2 + \Omega_2^2)}}, \tag{3.19}$$

and

$$k = \frac{(\Omega_0^2 - \Omega_2^2)}{(\Omega_0^2 + \Omega_2^2)}. \tag{3.20}$$

These parameters can be determined using the known values of Ω_0, Ω_1, and Ω_2, from the simulations, or by a cold test measurement in the laboratory. Here, we have used simulation tools for determining those parameters. An S-band reltron modulation section has been modeled in MAGIC [Goplen *et al.* (1995)] and CST MWS [CST Studio Suite (2020)] to obtain the normal modes at various coupling depths. The two software packages produced similar EM field patterns in all three modes, with a small difference in oscillation frequency as shown in Figure 3.5. The normal mode frequencies from MAGIC simulation, and the calculated ω_c, and k are listed in Table 3.1.

It can be observed from Figure 3.5 and Table 3.1 that, frequencies of both Ω_0 (0 mode) and Ω_1 ($\pi/2$ mode) decrease with d, but that of Ω_2 (π mode) increases, resulting in mode separation between 0 and π mode. This mode separation follows the analytical result of eqn. (3.15). As the coupling cavity approaches closer to the main cavity with increasing coupling depth d, the area of the coupling aperture increases. Hence, the coupling coefficient k is proportional to the coupling depth d. The variation of ω_c and k with d is shown in Figure 3.6. The frequency differences among the three modes are not equal, in general, because of the non-linear dependence, shown in equation (3.15).

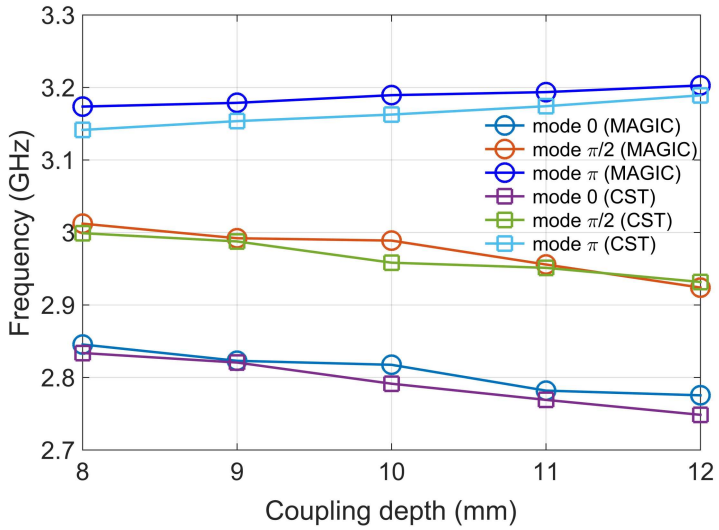

Figure 3.5: Mode frequencies at different (d) from CST MWS, and MAGIC.

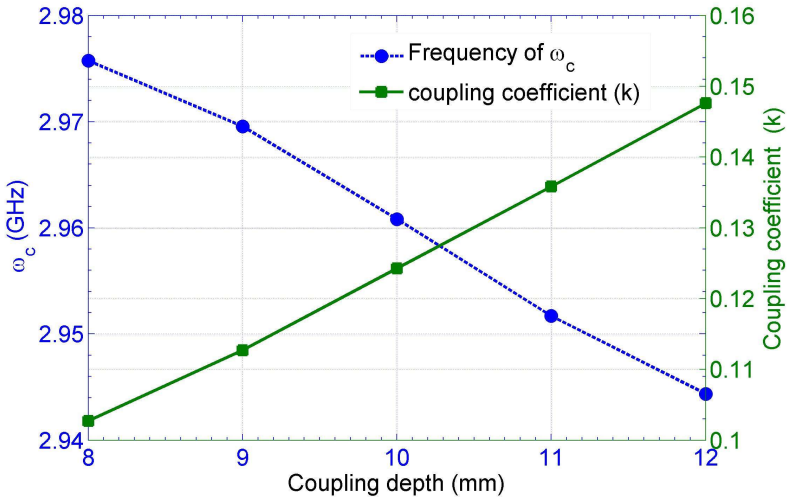

Figure 3.6: Variation of ω_c and k with coupling depth (d).

Table 3.1: Resonant frequencies at different d, and the corresponding ω_c and k.

Coupling depth d (mm)	Frequency (GHz) of mode $\Omega_0(0)$	$\Omega_1(\pi/2)$	$\Omega_2(\pi)$	ω_c (GHz)	k
8	2.833759	2.999028	3.141475	2.975750	0.103
9	2.820617	2.987673	3.153625	2.973225	0.111
10	2.791422	2.958359	3.162672	2.959725	0.124
11	2.769133	2.951259	3.174193	2.951014	0.136
12	2.748505	2.931753	3.189124	2.944370	0.148

3.5 Conclusion

The reltron's modulation section consists of three cavities, and it supports three normal modes; $0, \pi/2$, and π. The frequencies and the EM field patterns of these modes have been obtained and compared by using the two software packages, MAGIC and CST MWS. The frequency differences among these modes are not equal, and proper tuning is necessary for optimum performance. The increase in mode separation with coupling depth matched with the analytical result. The coupling coefficient increases monotonically as d increases. The resonant frequency of the on-axis cavities decreases, while that of the coupling cavity remains relatively constant.

CHAPTER iv

PIC Simulation and Results[†] [§]

Chapter index

[†]Part of this work has been published as: S. Shee, and S. Dwivedi, "Cold-test of reltron modulation section and PIC simulation study on output power and efficiency," *Int. J. RF Microw Comput Aided Eng.,* vol. 30, no. 3, doi:10.1002/mmce.22103

[§]Part of this work has been accepted for publication as: S. Shee, P. Tripathi, and S. Dwivedi, "Dispersion analysis of reltron modulation section and simulation study on the effect of coupling depth on device performance," *IEEE Trans. on Plas. Sci.*, doi:10.1109/TPS.2020.3000986